Associated Higgs boson production with a vector boson pair at hadronic supercolliders

Kingman Cheung
Department of Physics & Astronomy, Northwestern University, Evanston, Illinois 60208
(Received 25 October 1993)

We perform an exact calculation of the processes $pp \to W^+W^-H$, ZZH, $Z\gamma H$, $W^\pm ZH$, and $W^\pm\gamma H$ at hadronic supercolliders. They have sizable production cross sections of order 3–120 fb at the SSC and about 1–40 fb at the LHC for an intermediate mass Higgs (IMH) boson. They are higher order processes contributing to the IMH signals of WH, $t\bar{t}H \to \ell\nu\gamma\gamma X$ and $\ell\nu b\bar{b}X$. But they turn out to be relatively unimportant.

PACS number(s): 13.85.Qk, 14.70.Fm, 14.80.Bn

I. INTRODUCTION

The search for an intermediate mass Higgs (IMH) boson presents a challenge to the experimental development on the capability of the detector at both the Superconducting Super Collider (SSC) and CERN Large Hadron Collider (LHC). Namely, the studies [1] so far require a detector of extremely high invariant mass resolution for the $\gamma\gamma$ pair, which serves as the spectacular signature from the rare decay of an IMH boson. Recently, some studies [2] were carried out using the $H \to b\bar{b}$ mode under the presence of huge hadronic backgrounds, which relies very much on the B-tagging efficiencies of the vertex detectors.

The signals for the IMH boson in all these studies come from the production processes of $pp \to ZH$, WH, $t\bar{t}H$. At the SSC, the $t\bar{t}H$ cross section is about 1–1.5 times as much as the WH cross section, whereas at the LHC, the WH is about 1–2 times as much as the $t\bar{t}H$. The higher-order QCD correction to the WH and ZH has been shown to be small [3]. Because the signal is not large it is desirable to investigate higher-order productions of the Higgs boson that can contribute to the same final state or have other spectacular signatures. In this paper, we will investigate the associated production of a Higgs boson with a vector boson pair at hadronic supercolliders within the standard model (SM), via the subprocesses

$$q\bar{q} \to W^+W^-H\,, \tag{1}$$
$$q\bar{q} \to ZZH\,, \tag{2}$$
$$q\bar{q} \to Z\gamma H\,, \tag{3}$$
$$q\bar{q}' \to W^\pm ZH\,, \tag{4}$$
$$q\bar{q}' \to W^\pm\gamma H\,, \tag{5}$$

where q and q' represent different initial quark flavors. A naive estimation of these cross sections can be obtained by comparing with the three-vector boson productions at hadronic colliders [4] because the three-vector boson productions and the processes in (1) to (5) are of the same order in the weak coupling constant. It has been shown that the WWH, ZZH, and $Z\gamma H$ productions at e^+e^- collisions [5] are about 5 to 10 times smaller than the three-vector boson productions at e^+e^- collisions for the case of an IMH boson. Therefore, with cross sections of 0.1 – 1 pb for three-vector boson productions at the SSC [4], the cross sections for the processes in (1) to (5) are estimated to be tens to a hundred fb's.

All the processes in (1) to (5) can contribute to the $\gamma\gamma$ or $b\bar{b}$ signal of an IMH boson via the leptonic decay of either one of the vector bosons. These processes have an additional vector boson or photon that can be tagged on in order to eliminate certain types of backgrounds. In addition, through these processes the nonstandard HWW, HZZ, $H\gamma\gamma$, $HZ\gamma$ [6], and the anomalous quartic Higgs-gauge couplings, could be searched for. Furthermore, the ratio of the cross sections, e.g., $\sigma(WWH)/\sigma(ZZH)$, has the advantage that the uncertainties due to the structure functions, QCD corrections, and other systematic errors are reduced. But we also have to argue that these channels suffer severely from the QCD backgrounds at

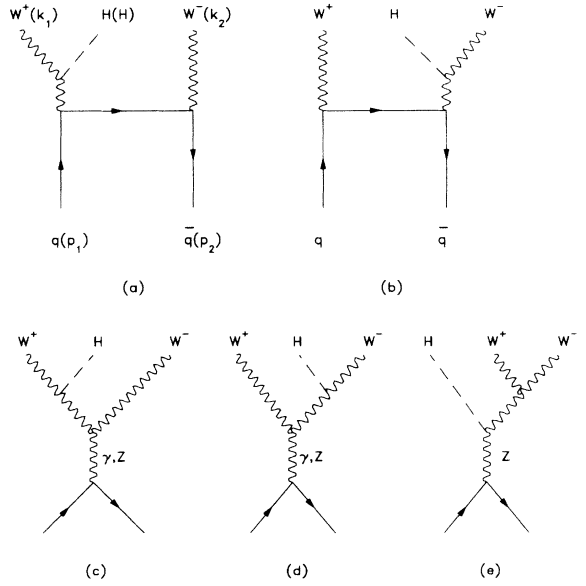

FIG. 1. The contributing Feynman diagrams for the subprocess $q(p_1)\,\bar{q}(p_2) \to W^+(k_1)\,W^-(k_2)\,H(H)$ in the unitary gauge, in which the unphysical Higgs bosons do not contribute.

hadronic supercolliders.

The organization is as follows: The calculation method will be illustrated in Sec. II, and the results will be presented in Sec. III, and we will conclude in Sec. IV.

II. CALCULATIONS

The contributing Feynman diagrams for the subprocess $q(p_1)\bar{q}(p_2) \to W^+(k_1)W^-(k_2)H(H)$, where the four-momenta of the particles are given in the parentheses, are shown in Fig. 1. Diagrams for the other processes can be written down similarly. We will use the helicity amplitude method of Ref. [7] to evaluate the Feynman amplitudes. We introduce the notation:

$$g_v^Z(q) = \frac{g}{\cos\theta_W}\left(\frac{T_{3q}}{2} - Q_q \sin^2\theta_W\right), \quad g_a^Z(q) = -\frac{g}{\cos\theta_W}\left(\frac{T_{3q}}{2}\right), \quad g_v^\gamma(q) = g\,\sin\theta_W(Q_q), \quad g_a^\gamma = 0\,,$$

$$g_v^W = -g_a^W = \frac{g}{2\sqrt{2}}, \quad g^V(q) = g_v^V(q) + g_a^V(q)\gamma^5,$$

$$g_{VWW} = \begin{cases} g\cos\theta_W & \text{if } V = Z, \\ g\sin\theta_W & \text{if } V = \gamma, \end{cases}$$

$$D^V(k) = 1/(k^2 - m_V^2), \quad P_{\mu\nu}^V(k) = \left(g_{\mu\nu} - \frac{k_\mu k_\nu}{m_V^2}\right),$$

$$\Gamma^\mu(k_1, k_2; \epsilon_1, \epsilon_2) = (k_1 - k_2)^\mu \epsilon_1\cdot\epsilon_2 + (2k_2 + k_1)\cdot\epsilon_1\epsilon_2^\mu - (2k_1 + k_2)\cdot\epsilon_2\epsilon_1^\mu,$$

$$J_{Vq}^\mu = \bar{v}(p_2)\gamma^\mu g^V(q)u(p_1)\,,$$

where g is the SU(2) gauge coupling, θ_W is the weak mixing angle, Q_q is the electric charge of the quark q in unit of proton charge, and T_{3q} is the third component of weak isospin of quark flavor q. Dots between four-vectors denote scalar products. For simplicity we present the helicity amplitude in the unitary gauge, in which the unphysical Higgs bosons do not contribute. The amplitudes of the corresponding Feynman diagrams (Fig. 1) are given by

$$i\mathcal{M}^{(a)} = -igm_W D^W(k_1 + H)\, P_{\mu\nu}^W(k_1 + H)\, \epsilon^\nu(k_1)\, \bar{v}(p_2)\not{\epsilon}(k_2) g^W \frac{\not{k}_2 - \not{p}_2}{(k_2 - p_2)^2}\gamma^\mu g^W u(p_1), \tag{6}$$

$$i\mathcal{M}^{(b)} = -igm_W D^W(k_2 + H)\, P_{\mu\nu}^W(k_2 + H)\, \epsilon^\nu(k_2)\, \bar{v}(p_2)\gamma^\mu g^W \frac{\not{p}_1 - \not{k}_1}{(p_1 - k_1)^2}\not{\epsilon}(k_1) g^W u(p_1), \tag{7}$$

$$i\mathcal{M}^{(c)} = \sum_{V=Z,\gamma} ig_{VWW} g m_W D^V(p_1 + p_2) D^W(k_1 + H)\, P_{\mu\nu}^W(k_1 + H)\, \epsilon^\nu(k_1)\, \Gamma^\mu(-k_2, p_1 + p_2; \epsilon(k_2), J_{Vq}), \tag{8}$$

$$i\mathcal{M}^{(d)} = \sum_{V=Z,\gamma} ig_{VWW} g m_W D^V(p_1 + p_2) D^W(k_2 + H)\, P_{\mu\nu}^W(k_2 + H)\, \epsilon^\nu(k_2)\, \Gamma^\mu(p_1 + p_2, -k_1; J_{Vq}, \epsilon(k_1)), \tag{9}$$

$$i\mathcal{M}^{(e)} = i\frac{g^2 m_W}{\cos\theta_W} D^Z(p_1 + p_2) D^Z(k_1 + k_2)\, J_{Vq}^\mu \Gamma_\mu(k_2, k_1; \epsilon(k_2), \epsilon(k_1)), \tag{10}$$

where $\epsilon(k_1)$ and $\epsilon(k_2)$ are the polarization four-vector of the W^+ and W^- bosons, respectively. Amplitudes for the other processes can be written down similarly. We will use the following parameters for numerical results: $m_Z = 91.175$ GeV and $\sin^2\theta_W = 0.23$, and m_W is generated in lowest order by $m_W = m_Z\cos\theta_W$. For the proton structure function we will use the Harriman-Martin-Roberts-Stirling (HMRS) (set B) [8] with $Q^2 = \hat{s}/4$, where $\hat{s}$ is the center-of-mass energy squared of the subprocess, and sum over u, d, s, c for the initial flavors. The productions of $W\gamma H$ and $Z\gamma H$ can be considered the photon bremsstrahlung of the WH and ZH productions, respectively. To visualize the final state photon we impose the acceptance cuts of

$$p_{T\gamma} > 25 \text{ GeV} \qquad \text{and} \qquad |\eta_\gamma| < 3 \tag{11}$$

on the transverse momentum $p_{T\gamma}$ and pseudorapidity η_γ of the final state photon. Later we will also show the difference when the CTEQ-1M [9] parton distributions are employed.

III. RESULTS

The dependence of the total cross sections of the processes in (1) to (5) on the center-of-mass energies of the pp system are shown in Fig. 2, for a typical Higgs boson mass of $m_H = 100$ GeV in the intermediate mass range. As expected, these cross sections increase with energy very rapidly at the small center-of-mass energies $\sqrt{s}$ and only as $\log(s)$ at higher $\sqrt{s}$. The WWH has the largest cross section of 47 and 14 fb for $m_H = 100$ GeV at the SSC and LHC, respectively. Considering the decay mode of $H \to b\bar{b}$, and the $\ell\bar{\nu}\bar{\ell}'\nu$, $\ell\nu jj$, and $jjjj$ decay modes of the WW, where $\ell, \ell' = e, \mu$ and j denotes a jet, we have about 18, 110, and 170 events for the corresponding $\ell\bar{\nu}\bar{\ell}'\nu b\bar{b}$, $\ell\nu jj b\bar{b}$, and $jjjj b\bar{b}$ final states for one SSC

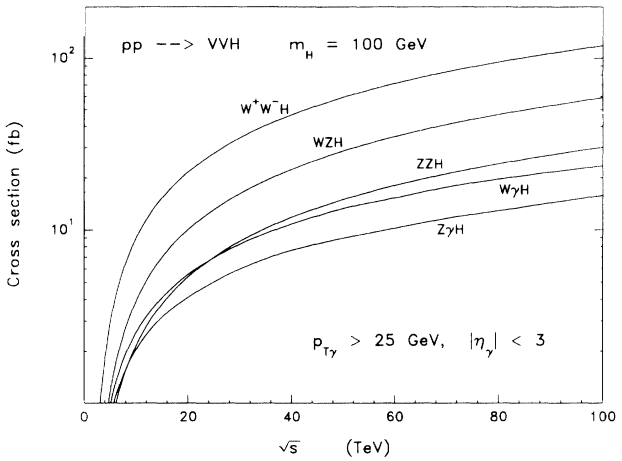

FIG. 2. Total cross sections for the processes $pp \to VVH$ versus the center-of-mass energies $\sqrt{s}$ for $m_H = 100$ GeV, with the acceptance cuts of $p_{T\gamma} > 25$ GeV and $|\eta_\gamma| < 3$ on the final state photon. The WZH and $W\gamma H$ include both the W^+ and W^- charge states.

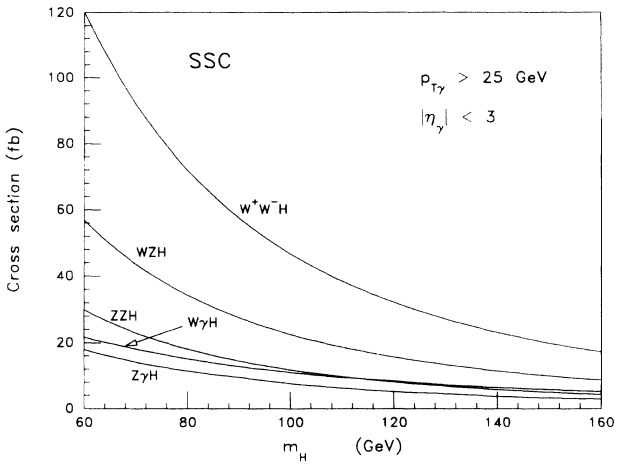

FIG. 3. The dependence of the total cross sections for the processes $pp \to VVH$ on the Higgs boson mass at the SSC energy (40 TeV), with the acceptance cuts of $p_{T\gamma} > 25$ GeV and $|\eta_\gamma| < 3$ on the final state photon. The WZH and $W\gamma H$ include both the W^+ and W^- charge states.

year (10 fb^{-1}), and about three times as much for one LHC year (100 fb^{-1}). The WZH and ZZH have the second and third largest cross sections except at the very small $\sqrt{s}$, at which the phase space to produce the ZZH is much smaller than the $W\gamma H$. The $W\gamma H$ and $Z\gamma H$ have the smallest cross sections due to the acceptance cuts imposed on the final state photon, and also due to the absence of the tree-level coupling of the Higgs bosons and photons.

Another interesting feature is the ratio of the $\sigma(WWH)$:$\sigma(WZH)$:$\sigma(ZZH)$, which is about 4:2:1 at very large $\sqrt{s}$ due to the SM values of HWW and HZZ couplings. This ratio is more reliable at very high energy, for the sea-quark partons are much more important than the valence ones in the small x region. Assuming the flavor symmetry in the sea-quark distributions, the factors from the initial parton distributions are the same for the WWH, WZH, and ZZH productions, e.g., $u\bar{u} \approx u\bar{d}$, $c\bar{c} \approx c\bar{s}$. So the ratio $\sigma(WWH)$:$\sigma(WZH)$:$\sigma(ZZH)$ would be different from the SM prediction if the HWW and HZZ couplings deviate sufficiently from their SM values. Or if the HWW and HZZ couplings are assumed the SM values, this ratio will give some hints on the flavor asymmetries in the sea-quark distributions.

The variation of the cross sections with the Higgs boson mass m_H in the intermediate mass range at the SSC and LHC are shown in Figs. 3 and 4, respectively. We can see that the productions at $m_H = 60$ GeV are about 2–3 times as much as those at $m_H = 100$ GeV, and at $m_H = 160$ GeV the productions are about 1/2 of those at $m_H = 100$ GeV.

We show in Table I the comparison between the HMRS (set B) and the CTEQ-1M in the productions of VVH for a few m_H values at the SSC and LHC. Overall the CTEQ-1M gives larger cross sections by about a few to 40 %, with the largest difference at the smaller Higgs boson masses and at the higher energies. This implies larger uncertainties of the sea-quark parton distributions at the smaller x.

IV. DISCUSSIONS

One of the reasons to investigate these VVH productions is to see how much they can contribute to the IMH signals at the future SSC and LHC. The signals for the IMH boson search at hadronic colliders are ℓHX followed by $H \to \gamma\gamma$ [1] or $b\bar{b}$ [2]. The total production cross section of ℓHX from the processes (1) to (5) is about 32 fb for $m_H = 100$ GeV at the SSC with HMRS (set B). Comparing to the $\sigma(pp \to WH, ZH \to \ell HX)$ (~ 1.6 pb), the increase to the ℓHX signal due to the processes

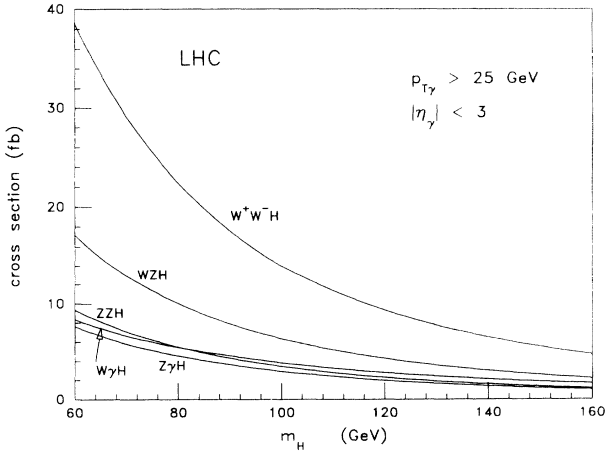

FIG. 4. The dependence of the total cross sections for the processes $pp \to VVH$ on the Higgs boson mass at the LHC energy (14 TeV), with the acceptance cuts of $p_{T\gamma} > 25$ GeV and $|\eta_\gamma| < 3$ on the final state photon. The WZH and $W\gamma H$ include both the W^+ and W^- charge states.

TABLE I. The comparison between the parton distributions HMRS (set B) and CTEQ-1M in the production cross sections (fb) of $pp \to VVH$ for m_H=60, 100, and 160 GeV at the SSC and LHC, with the acceptance cuts of $p_{T\gamma} > 25$ GeV and $|\eta_\gamma| < 3$ on the final state photon. The first column gives the HMRS and the second gives the CTEQ-1M. The numbers in the parentheses are for the LHC (14 TeV).

m_H	WWH		WZH		ZZH		$W\gamma H$		$Z\gamma H$	
	HMRS	CTEQ	HMRS	CTEQ	HMRS	CTEQ	HMRS	CTEQ	HMRS	CTEQ
60	120	170	57	75	30	43	22	30	18	25
	(39	47)	(17	20)	(9.3	12)	(8.4	10)	(7.6	9.3)
100	47	63	22	29	12	16	11	15	7.6	10
	(14	17)	(6.3	7.1)	(3.5	4.1)	(3.8	4.5)	(2.9	3.5)
160	17	22	8.6	11	4.3	5.8	5.1	6.7	2.9	3.8
	(4.7	5.2)	(2.2	2.4)	(1.2	1.3)	(1.7	1.8)	(1.0	1.2)

in (1) to (5) is only 2%. This is already smaller than the QCD correction ($\lesssim 10\%$) to the WH and ZH productions [3]. Therefore, in terms of contributing to the IMH boson signal, the processes under consideration are relatively unimportant.

On the other hand, the processes in (1) to (5) have their own spectacular signature. Because the production rates are small, these rare processes will only be searched for after the discovery of the Higgs boson. The presence of anomalous HVV ($V = \gamma, Z, W$) couplings might change the production rates of certain channels, especially, the $W\gamma H$ and $Z\gamma H$ channels could be enhanced significantly by the anomalous tree-level $HZ\gamma$ and $H\gamma\gamma$ couplings. However, the enormous large $t\bar{t}$ and the three-vector boson productions present major obstacles for observing these rare processes when the $H \to b\bar{b}$ decay mode is considered. The $t\bar{t}$ so produced decay almost 100% into $b\bar{b}WW$, which gives a cross section in the order of 10 nb at the SSC, and so it completely buries the small WWH, WZH, and ZZH signal, unless the mass reconstructions of the W, Z, H, and t are accurate enough to distinguish among the W, Z, and H, and to reject the $t\bar{t}$ events with $m(bW) \approx m_t$. But the experimental situation at the hadronic supercolliders hardly makes it possible. For the $pp \to W\gamma H$ and $Z\gamma H$ processes the backgrounds come from $t\bar{t}\gamma$, $WW\gamma$, $WZ\gamma$, and $ZZ\gamma$, which are more than an order of magnitude larger. Therefore, all the processes under consideration with the decay mode $H \to b\bar{b}$ suffer severely from the $t\bar{t}$ and related backgrounds, and the three-vector boson backgrounds. Summing up, it does not seem feasible to use these processes to search for the anomalous HVV couplings and the quartic Higgs-gauge couplings.

In conclusion, we have performed an exact calculation of the tree-level productions $pp \to VVH$ for the case of IMH boson. The production rates are sizable and are about tens to a hundred fb's at the SSC and about 1/3 of this at the LHC. As higher-order corrections to the IMH boson signal of ℓHX, these processes give a total of only 2% increase to $WH, ZH \to \ell HX$. Also these rare processes are hard to be observed due to the huge $t\bar{t}$ and the three-vector boson productions, and due to the lack of very accurate mass reconstructions at the hadronic environment.

ACKNOWLEDGMENTS

This work was supported by the U.S. Department of Energy, Division of High Energy Physics, under Grant No. DE-FG02-91-ER40684.

[1] See, e.g., SDC Technical Design Report No. SDC-92-201 (unpublished).

[2] T. Garavaglia, Wai-kwok Kwong, and Dan-Di Wu, Phys. Rev. D **48**, R1899 (1993); J. Dai, J. F. Gunion, and R. Vega, Phys. Rev. Lett. **71**, 2699 (1993).

[3] T. Han and S. Willenbrock, Phys. Lett. B **273**, 167 (1992); J. Ohnemus and W.J. Stirling, Phys. Rev. D **47**, 2722 (1993); H. Baer, B. Bailey, and J.F. Owens, *ibid.* **46**, 2730 (1993).

[4] M. Golden and S.R. Sharpe, Nucl. Phys. **B261**, 217 (1985); V. Barger and T. Han, Phys. Lett. B **212**, 117 (1988).

[5] M. Baillargeon *et al.*, CERN Report No. CERN-TH.6932/93 (unpublished).

[6] K. Hagiwara, R. Szalapski, and D. Zeppenfeld, Phys. Lett. B **318**, 155 (1993).

[7] V. Barger, A. Stange, and R. J. N. Phillips, Phys. Rev. D **44**, 1987 (1991).

[8] P. N. Harriman *et al.*, Phys. Rev. D **42**, 798 (1990).

[9] CTEQ Collaboaration, J. Botts *et al.*, Phys. Lett. B **304**, 159 (1993).